Biochimica et Biophysica Acta 858 (1986) 221–234
Elsevier

BBA 72925

Evidence that pyrene excimer formation in membranes is not diffusion-controlled

Mary F. Blackwell, Kleoniki Gounaris and James Barber

Department of Pure and Applied Biology, Imperial College, London SW7 2BB (U.K.)

(Received February 24th, 1986)

Key words: Pyrene excimer; Fluorescence; Liposome; Lateral diffusion

Kinetic and steady-state measurements of pyrene fluorescence in a variety of model membranes are evaluated in terms of the theory of collisional excimer formation. In the region of 10^{-3}–0.1 M pyrene, molecular fluorescence decay in membranes is biphasic and the two component lifetimes do not depend on the pyrene concentration. The lifetime data are consistent with the rate constant for collisional excimer formation being of the order 10^6 $M^{-1} \cdot s^{-1}$ or less. The concentration dependence of the component amplitudes is inconsistent with the theory of collisional excimer formation and suggests that pyrene exists in two forms in membranes: a slowly diffusing monomeric form and an aggregated form. The component of molecular fluorescence decay associated with aggregated pyrene is highly correlated with steady-state excimer fluorescence, suggesting that excimer fluorescence in membranes arises from aggregated pyrene in which excimers are formed by a static rather than a collisional mechanism. It is suggested that the concentration dependence of excimer to molecular fluorescence intensity ratios in membranes is related to the equilibrium constant for exchange between monomeric and aggregated pyrene forms rather than to the collisional excimer formation rate constant.

Introduction

Pyrene is the classical example of molecules that form excited-state dimers (excimers) [1–3]. Excimer formation is a bimolecular reaction; thus, if it is diffusion-controlled, the reaction rate constant can be related to the diffusion coefficient of pyrene and the viscosity of the solvent [3]. Pyrene fluorescence kinetics in organic solvents are described well by a theoretical model of collisional excimer formation [1–3]. The model predicts a particular functional dependence of the kinetic parameters on the pyrene concentration when the reaction is diffusion-controlled. Thus, a collisional mechanism of excimer formation can readily be established by studying the concentration dependence of the rate parameters.

Pyrene excimer formation in aqueous dispersions of lipids or detergents has been used to estimate lateral diffusion coefficients of pyrene [5–11] and lipid-pyrene adducts [8]. It has been assumed in most studies that excimer formation is a diffusion-controlled reaction in membranes. This assumption was extrapolated from the studies in organic solvents and has not been adequately tested by means of studies of the concentration dependence of fluorescence-decay kinetics. We have therefore studied pyrene fluorescence kinetics in several model membrane systems to evaluate the validity of the technique in terms of the theory of collisional excimer formation.

Theoretical section

The theory of collisional excimer formation

Table I summarizes the analysis developed by

Birks and coworkers [1–3] to describe collisional excimer formation. M and D denote monomers and dimers, and asterisks denote excitation. The kinetics depend on four parameters: the monomer and excimer fluorescence-decay constants, k_M and k_D; the second-order rate constant of excimer formation, k_{DM}; and the excimer dissociation rate constant, k_{MD}. The excitation intensity is considered to be low enough that the concentration of ground-state pyrene is independent of time so that

TABLE I

SUMMARY OF THE THEORY OF COLLISIONAL EXCIMER FORMATION

For details, see Refs. 1–3. c_X = molar concentration of X. $I_{M(D)}(t)$ = intensity of molecular (excimer) fluorescence at time t. $\Phi_{M(D)}$ = molecular (excimer) fluorescence quantum yield.

Kinetic scheme

Process	Description	Rate parameter
(1) $M^* \rightarrow M + h\nu_M$	monomer fluorescence	k_{fM}
(2) $M^* \rightarrow M$	monomer radiationless deactivation	k_{iM} } k_m } X
(3) $M^* + M \rightarrow D^*$	excimer formation	$k_{DM}c_M$
(4) $D^* \rightarrow M + M + h\nu_D$	excimer fluorescence	k_{fD}
(5) $D^* \rightarrow M + M$	excimer radiationless deactivation	k_{iD} } k_D } Y
(6) $D^* \rightarrow M^* + M$	excimer dissociation	k_{MD}

Rate equation

$$\frac{d}{dt}\begin{pmatrix} c_{M^*} \\ c_{D^*} \end{pmatrix} = R\begin{pmatrix} c_{M^*} \\ c_{D^*} \end{pmatrix}, \text{ where } R = \begin{pmatrix} -X & k_{MD} \\ k_{DM}c_M & -Y \end{pmatrix} \tag{7}$$

Eigenvalues of R

$$T_{1,2}^{-1} = R_{1,2} = \tfrac{1}{2}\left(X + Y \mp \left((Y-X)^2 + 4k_{MD}k_{DM}c_M \right)^{1/2} \right) \tag{8}$$

Solutions

$$\frac{I_M(t)}{I_M(0)} = A_1 e^{-t/T_1} + A_2 e^{-t/T_2};\ A_1 = \frac{R_2 - X}{R_2 - R_1},\ A_2 = \frac{X - R_1}{R_2 - R_1} \tag{9}$$

$$\frac{I_D(t)}{I_M(0)} = \frac{k_{DM}c_M}{R_2 - R_1}\left(e^{-t/T_1} - e^{-t/T_2} \right) \tag{10}$$

Concentration dependence and asymptotic values

$$\frac{d(R_1 + R_2)}{dc_M} = k_{DM} \tag{11}$$

$c_M \rightarrow 0$	(12)	$c_M \rightarrow \infty$	(13)
$T_1 \rightarrow k_M^{-1}$		$T_1 \rightarrow k_D^{-1}$	
$T_2 \rightarrow Y^{-1}$		$T_2 \rightarrow (k_D + X)^{-1}$	
$A_1 \rightarrow 1$		$A_1 \rightarrow 0$	
$A_2 \rightarrow 0$		$A_2 \rightarrow 1$	

Steady-state solution [a]

$$\frac{\Phi_D}{\Phi_M} = \frac{k_{fD}k_{DM}c_M}{k_{fM}(k_D + k_{MD})} \tag{14}$$

[a] Obtained from the solution of Eqn. 7 assuming photostationary conditions.

$k_{DM}c_M$ is a pseudo-first-order rate constant. Excimer formation kinetics can then be represented by a rate matrix, R in Eqn. 7, and the fluorescence lifetimes T_1 and T_2 are determined by diagonalization. Theoretical expressions for time-dependent monomer and excimer fluorescence intensities, $I_M(t)$ and $I_D(t)$, respectively, are obtained from the eigenvectors of R and are given in Eqns. 9 and 10.

Vanderkooi and Callis [5] pointed out that in highly viscous media it may be improper to neglect the time dependence of the excimer formation reaction rate and they used an equation of the form

$$I_M(t) = I_M(0) \exp - \left(k_M + \left[1 + a(\pi Dt)^{-1/2}\right] k_{DM}c_M\right)t \qquad (9')$$

rather than Eqn. 9 to describe molecular fluorescence decay kinetics, with a the interaction radius (0.5–1 nm) and D the pyrene diffusion coefficient. They suggested that the $t^{1/2}$ term accounts for nonexponentiality of pyrene molecular fluorescence decay rather than biexponential kinetics and they assumed $k_{MD} = 0$. We feel that their treatment is incorrect for the following reasons. It is easy to see by inspection of R in Table I that if k_{MD} is zero, monomer and excimer fluorescence kinetics are uncoupled and, as a result, this model cannot describe biphasic molecular fluorescence kinetics, even when the amplitudes A_1 and A_2 in Eqn. 9 are not near their asymptotic values in Eqns. 12 and 13. Eqn. 9′ is based on the theory of bimolecular reactions in isotropic media [12] and although the theory for anisotropic media [13] is more complicated, when D is of the order 10^{-8} $cm^2 \cdot s^{-1}$ or less, the isotropic theory will be approximately correct in anisotropic media throughout the pyrene fluorescence lifetime. It is straightforward to show that the time dependence of the reaction rate is accounted for by multiplying the right sides of Eqns. 9 and 10 by $\exp(-k_{DM}ac_M[t/\pi D]^{1/2})$ and $\exp(k_{DM}ac_M[t/\pi D]^{1/2})$, respectively. Thus, the model in Table I remains valid when the reaction rate is time-dependent. Moreover, the exponential correction factors are within 2% of unity throughout the pyrene fluorescence lifetime, even when k_{DM} and D are as low as 10^5 $M^{-1} \cdot s^{-1}$ and 10^{-10} $cm^2 \cdot s^{-1}$, respectively, at pyrene concentrations as high as 0.1 M. We therefore neglect the time dependence of the excimer formation reaction rate.

Experimental tests of diffusion control

Birks et al. [1–3] described the criteria for establishing that pyrene excimer formation is a diffusion-controlled reaction. Firstly, to establish that excimer formation results from collisional encounters it is necessary to demonstrate that the concentration dependence required by the model in Table I is satisfied. Secondly, in order to establish that the reaction is under diffusional rather than chemical control, it is necessary to demonstrate that the second-order rate constant of excimer formation, k_{DM}, has the same value and the same viscosity and temperature dependence as the theoretical molecular collision parameter, calculated in isotropic media by means of the Stokes-Einstein and Einstein-Smoluchowski theories [3].

The concentration dependence of fluorescence kinetics in collisional excimer formation. It is evident in Fig. 1 that the lifetimes and amplitudes are independent of the concentration except for relatively sharp transitions which occur in regions where the cross term $4k_{MD}k_{DM}c_M$ in Eqn. 8 becomes comparable to the diagonal elements of R. Outside these transition regions, the amplitudes and lifetimes approach their asymptotic values, given in Eqns. 12 and 13 of Table I. The transitions are essentially complete within one or two orders of magnitude change in concentration. Transitions similar to the ones in Fig. 1 can be expected whenever $k_D > k_M$. The transitions may be characterized by the concentration, $c_{1/2}$ at which half the total change occurs.

Fig. 1 illustrates that k_{DM} influences primarily the $c_{1/2}$ values of the curves, whereas k_{MD} influences $c_{1/2}$ values and to some extent, the shapes of the curves. Fig. 1A and B shows that if k_{DM} alone is decreased by an order of magnitude, the $c_{1/2}$ values increase by an order of magnitude but the curves do not change shape. This is true regardless of the values of k_{MD}. Fig. 1C and D shows that so long as k_{MD} is of the order of magnitude of k_M and k_D or smaller, it has little influence on the shape of the concentration curves

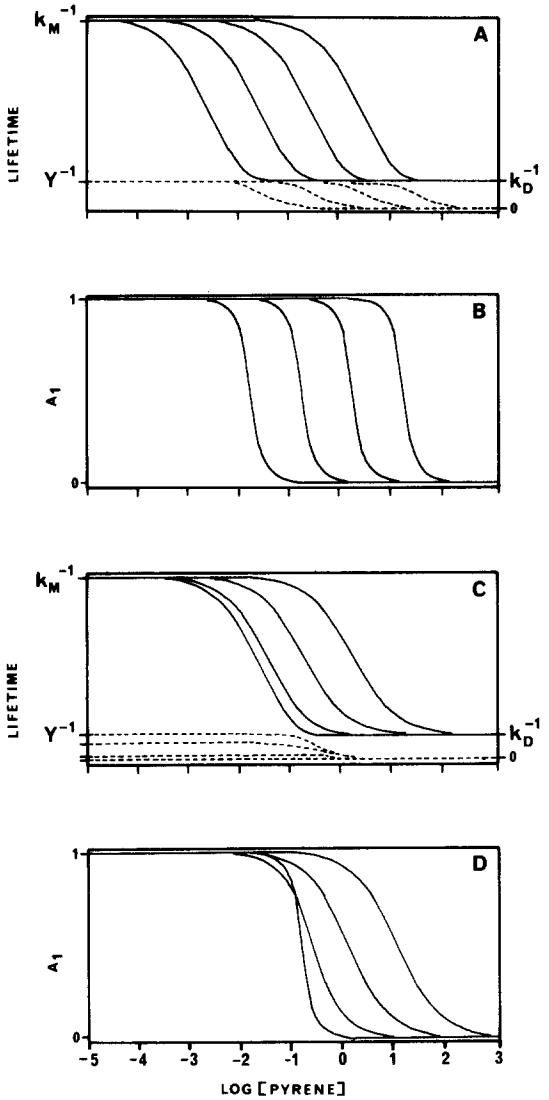

Fig. 1. Semi-log plots of theoretical pyrene concentration curves for the lifetimes T_1 and T_2, and slow phase amplitude A_1, of pyrene molecule fluorescence decay, calculated using Eqns. 8 and 9 of Table I. A, C: concentration dependences of T_1 (solid curves) and T_2 (dashed curves). B, D: concentration dependence of A_1. All symbols are defined in Table I. In A and C, k_M^{-1} and k_D^{-1} correspond to the asymptotic values of T_1 at low and high concentrations, respectively, and $Y^{-1} = (k_D + k_{MD})^{-1}$ corresponds to the asymptotic value of T_2 at low pyrene concentrations, shown in Eqns. 12 and 13 of Table I. The curves in A and B were calculated with $k_{MD} = 10^6$ s^{-1} and $k_{DM} = 10^6$, 10^7, 10^8, and 10^9 $M^{-1} \cdot s^{-1}$ from right to left. The curves in C and D were calculated with $k_{DM} = 10^8$ $M^{-1} \cdot s^{-1}$ and $k_{MD} = 10^6$, 10^7, 10^8, 10^9 s^{-1} from left to right for T_1 and A_1 and from top to bottom for T_2. The values $k_M = 2.22 \cdot 10^6\ s^{-1}$ and $k_D = 1.55 \cdot 10^7\ s^{-1}$ for pyrene in cyclohexane were used in the calculation.

for T_1 and T_2. When k_{MD} becomes larger than k_M and k_D the transitions broaden somewhat for the amplitudes and T_1 and the $c_{1/2}$ values increase. The $c_{1/2}$ value for T_2 is independent of the relative magnitude of k_{MD}, but the asymptotic value of T_2 as $c_M = 0$ will obviously be affected according to Eqn. 12. However, it is not likely to be the case that $k_{MD} \gg k_M$, k_D, k_{DM} in membranes. The molecular equilibrium constant for excimer formation, k_{DM}/k_{MD}, is of the order 10^{-3} M^{-1} in organic solvents and is independent of environment [3]. Both k_{DM} and k_{MD} have Arrhenius-type temperature dependences, i.e.,

$$k_{DM} = k_{DM'} \exp(-E_f/RT)$$

$$k_{MD} = k_{MD'} \exp(-E_d/RT) \qquad (15)$$

and the activational barriers to excimer formation (E_f) and dissociation (E_d) have been observed to be influenced in similar ways by environmental factors, thus conserving the value of the equilibrium constant [3].

Based on this analysis, we make the following general statements about the concentration dependence of collisional excimer formation: (1) the amplitudes A_1 and A_2 and lifetimes T_1 and T_2 should display sharp transitions qualitatively similar to those in Fig. 1 with $c_{1/2}$ values that reflect the magnitude of the excimer formation rate constant k_{DM}, so long as k_{MD} is not much larger than k_D and k_M, and $k_D > k_M$; and (2) in any case, the concentration curve for the lifetime T_2 will indicate the order of magnitudes of both k_{MD} and k_{DM}.

The value of the theoretical molecular collision rate parameter for pyrene in membranes. Birks and coworkers [1–3] found that the values of k_{DM} in cyclohexane agree closely with the theoretical molecular collision rate parameter, K, calculated from the Stokes-Einstein and Einstein-Smoluchowski theories

$$K = 8RTpa/3000\,\mu b \qquad (16)$$

with μ the viscosity of the suspending medium, a the interaction radius, p the reaction probability per collision and b the Stokes radius. They found that for pyrene, $pa/b = 1$ [3]. The temperature dependence of k_{DM} and K in a variety of organic

solvents yields identical activation energies [3], i.e.,

$$K \approx K' \exp(-E_f/RT) \quad (17)$$

with E_f as defined for Eqn. 15, further supporting the argument that excimer formation in organic solvents is diffusion-controlled.

The activational barrier to pyrene diffusion in hydrocarbon solvents is in the region 10–15 kJ · M^{-1} [3,10]. Dorrance and Hunter [9–11] determined that the activational barrier to pyrene diffusion was 35 kJ · M^{-1} in cationic detergent micelles, 37 kJ · M^{-1} in aqueous dipalmitoylphosphatidylcholine (DPPC) dispersions, and 39 kJ · M^{-1} in aqueous dispersions of egg yolk PC. Based on differences in diffusional barriers, we would estimate the theoretical molecular collision parameter in membranes, K_m, to be of the order

$$K_m \approx K \exp((E_f - E_{fm})/RT) \quad (18)$$

with E_{fm} the activational barrier to diffusion in the membrane. At 298 K, RT is 2.48 kJ · M^{-1}. Calculating the largest and smallest values of the exponential factor in Eqn. 18, we estimate that at 298 K, K_m will be smaller than K by a factor in the region $8.3 \cdot 10^{-6}$–$1.4 \cdot 10^{-4}$. Since K for pyrene in cyclohexane is $6.7 \cdot 10^9$ $M^{-1} \cdot s^{-1}$, we estimate that K_m in membranes will be in the region $6 \cdot 10^4$–$1 \cdot 10^6$ $M^{-1} \cdot s^{-1}$ at 298 K. This would result in the observation of concentration dependence in the lifetimes and amplitudes at concentrations higher than those achievable in membranes. Eqn. 18 does not take into account differences in the theoretical expressions arising from the anisotropy of diffusion in membranes, but these should not change the order of magnitude of K_m. A more serious source of error in Eqn. 18 is that it does not include effects of changes in viscosity on the preexponential factor K' in Eqn. 17. Thus K_m in Eqn. 18 should be regarded as an upper limit, since the membrane viscosity is likely to be larger than that of cyclohexane.

The model in Table I imposes the following additional constraints on the observed kinetics if pyrene excimer formation in membranes involves a mechanism of collisional encounters: (1) the lifetimes T_1 and T_2 should be the same for both monomer and excimer fluorescence kinetics, according to Eqns. 9 and 10; and (2) the lifetimes should satisfy the dependence on the concentration of ground-state pyrene given in Eqn. 11. We note that failure to satisfy the theoretical criteria would mean that the relationship between steady-state molecular and excimer fluorescence intensities and k_{DM} given in Eqn. 14 is not applicable, since Eqn. 14 is derived from Eqn. 7 assuming photostationary conditions.

Experimental section

Material and Methods

Soya bean PC (99%), egg yolk PC (99%) and pyrene from Sigma Chemical Company Ltd. and soya bean asolectin from Associated Concentrates were used as purchased. Total polar lipid extracts of spinach chloroplast thylakoid membranes were isolated according to a procedure described elsewhere [14]. Neutral lipids and pigments were removed from the lipid extracts by column and thin-layer chromatography [15]. Thylakoid membrane PC was purified from total polar lipid extract by thin-layer chromatography. Where noted, catalytic hydrogenation was carried out as previously described [16]. Lipids were quantified by gas-liquid chromatography according to the method in Ref. 17.

Aqueous lipid dispersions were prepared as follows. Appropriate amounts of lipid and pyrene were combined from stock solutions and the solvent was evaporated under a stream of nitrogen. The mixtures were taken up in chloroform, dried under nitrogen and finally taken up in diethyl ether. After complete evaporation of the solvent the mixtures were dispersed in distilled water (pH 5) by ultrasonication in a water bath. Under these conditions, we expect aqueous lipid dispersions to consist of liposomes in a broad distribution of sizes, including both uni- and multilamellar vesicles (see Refs. 18, 19). All samples were placed in quartz cuvettes fitted with Subaseal rubber stoppers and bubbled with nitrogen for 10 min prior to fluorescence measurements.

Fluorescence measurements were made at room temperature (20°C). Steady-state emission was measured using a model MPF 44A spectrophotometer from Perkin Elmer. Kinetics were measured using a model SP-70 Nanosecond Fluores-

cence Spectrometer from Applied Photophysics Ltd. The full width at half maximum of the excitation flashes was 3–4 ns. Monochromators selected wavelengths for excitation (340 nm) and emission (390 nm for molecular and 480 nm for excimer fluorescence). Decay curves were transmitted to a Vector 3 microcomputer from Vector Graphics Inc. for analysis.

Results

Evidence that pyrene is incorporated into liposomes. It has usually been assumed [4–6,9,11,15] that pyrene partitions completely into the lipid phase of aqueous lipid dispersions. Dembo et al. [7] determined the partition coefficient of pyrene in erythrocyte membranes to be $7 \pm 2 \cdot 10^4$ at room temperature. Jones and Lee [20] used a centrifugation assay to determine the binding of pyrene and pyrene derivatives to PC membranes. They assumed that pyrene remaining in the supernatant after high-speed centrifugation was not associated with lipid. Under our experimental conditions, with lipid-to-pyrene molar ratios in the region 100–500, we found that 10–30% of pyrene fluorescence remains in the supernatant after high-speed centrifugation of aqueous lipid dispersions. It seemed unlikely to us that such a high percentage of pyrene would remain in the aqueous phase. We therefore determined the lipid content of supernatants and pellets after centrifugation of soya bean PC liposomes at $175\,000 \times g$ for 1.5 h. We found that pyrene in the supernatants is associated with lipid in the same lipid/pyrene ratio as in the original suspensions and the pellets.

Fluorescence spectra also suggest that aqueous pyrene does not contribute significantly to pyrene fluorescence in aqueous lipid dispersions. Fig. 2 shows steady-state fluorescence emission spectra of 0.25 μM pyrene in distilled water and in an aqueous suspension of 0.25 $mg \cdot ml^{-1}$ soya bean PC. It is evident that the fluorescence emission of pyrene in water differs markedly from that of pyrene in aqueous lipid dispersions in the relative intensities of the vibronic transitions; e.g., the transition at 375 nm is more intense than the transition at 398 nm in water, whereas the reverse is true in lipid dispersions. Changes in the relative intensities of vibronic transitions in response to changes in solvent polarity ('Ham effects') are

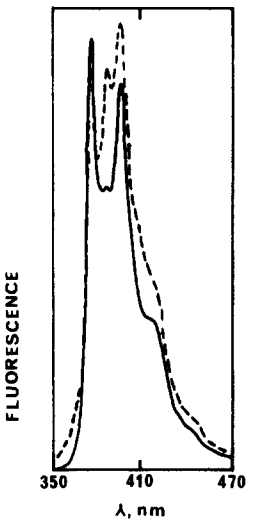

Fig. 2. Fluorescence emission at 20°C from 0.25 μM pyrene in distilled water on a 0.1 V scale (solid line) and in an aqueous dispersion of 0.25 $mg \cdot ml^{-1}$ soya bean PC on a 0.2 V scale (dashed line). Fluorescence was excited at 340 nm.

characteristic of aromatic hydrocarbons like pyrene [11,21]. Taking the ratio $R_H = I_{385}/I_{398}$ to indicate the magnitude of the Ham effect, we found that $R_H = 0.92 \pm 0.03$ for pyrene in water, whereas $R_H = 1.09 \pm 0.01$ for pyrene in dispersions of soya bean PC and in both supernatant and pelleted material after centrifugation at $175\,000 \times g$.

As found by Jones and Lee [20], the fluorescence emission of pyrene in Fig. 2 is more intense in aqueous lipid dispersions than in water. The fluorescence intensity of pyrene in liposomes can be as much as 4-times greater than that of the same concentration of pyrene in water [20]. This effect will also tend to diminish the relative contribution of fluorescence from any aqueous pyrene.

Concentration studies of pyrene fluorescence kinetics. We studied the effect of the pyrene concentration on fluorescence kinetics in aqueous suspensions of the following lipids: soya bean asolectin (five experiments), thylakoid membrane total polar lipids (three experiments), thylakoid membrane PC (three experiments), and soya bean or egg yolk PC (five experiments). We also studied thylakoid PC which had been subjected to catalytic hydrogenation and had a double-bond index

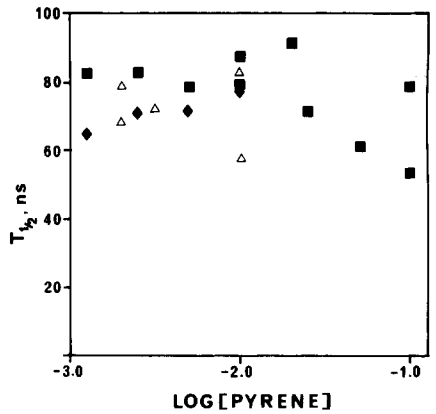

Fig. 3. The concentration dependence of the halftime of pyrene molecular fluorescence decay at 20°C in aqueous dispersions of thylakoid total polar lipid extract (△), thylakoid PC with a double-bond index of 3.7 (■) and hydrogenated thylakoid PC with a double-bond index of 0.2 (◆). Fluorescence was excited at 340 nm and measured at 390 nm.

of 0.2, compared with 3.7 in untreated thylakoid PC. The fatty acid composition of this preparation was 76% stearic acid and 24% palmitic acid. We estimated the concentration of pyrene in the lipid phase via the following equation

$$(\text{mmol pyrene})\,(\text{ml lipid})^{-1} = M_P D_L m_L^{-1} \cdot 10^3 \qquad (19)$$

where M_P is the molarity of pyrene in the suspension in units of mol $\cdot$ l^{-1}, D_L is the lipid density in the liposomes in units of g $\cdot$ ml^{-1}, and m_L is the molality of lipid in the suspension in units of g $\cdot$ l^{-1}. Eqn. 19 assumes a high partition coefficient for pyrene between the lipid and aqueous phases, and we assumed a value of unity for D_L [18,19].

Fig. 3 shows the effect of the pyrene concentration on the halftime of molecular fluorescence decay in normal and hydrogenated thylakoid PC liposomes and in liposomes of thylakoid total polar lipids. There is no obvious concentration dependence of the decay kinetics in the concentration region 10^{-3}–10^{-1} M pyrene. Indeed, we did not observe an obvious concentration dependence of fluorescence kinetics in any of the lipids we studied, and often found that the kinetic traces at

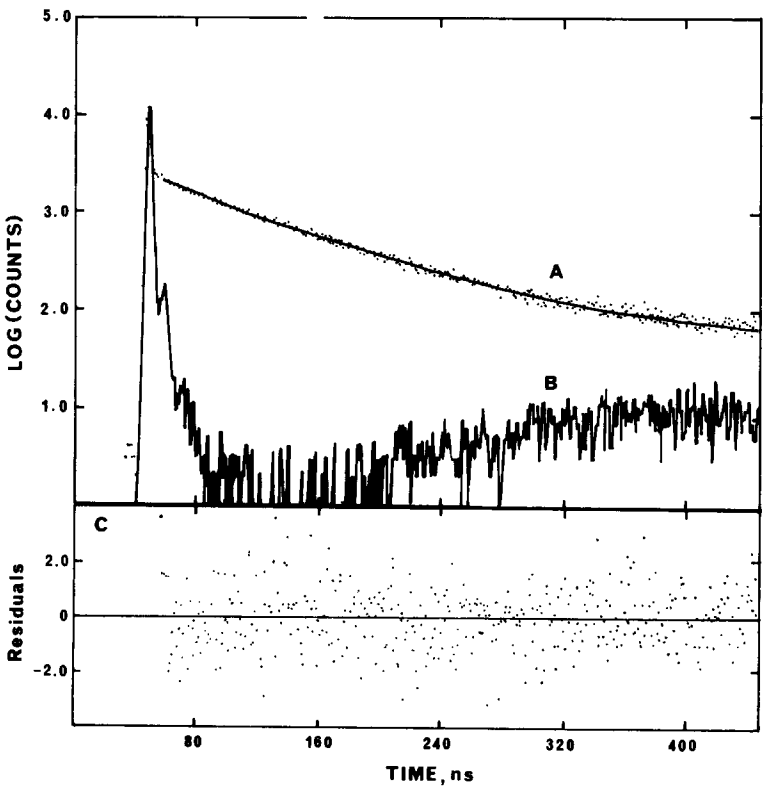

Fig. 4. Semi-log plot of the molecular fluorescence kinetics of 0.5 μM pyrene in an aqueous dispersion of 0.2 mg $\cdot$ ml^{-1} soya bean PC. A: dots, experimental decay data; solid curve, theoretical decay obtained from deconvolution of the lamp profile combined with least-squares analysis assuming two exponential components. B: lamp profile. C: residuals of the least-squares analysis. Measurement conditions were the same as in Fig. 3.

the high and low ends of the concentration range were virtually superimposable.

Fig. 4 shows molecular fluorescence kinetics in a suspension of 0.50 μM pyrene and 0.20 mg · ml^{-1} soya bean PC. The solid curve in Fig. 4A is the theoretical decay curve obtained from deconvolution of the emission (Fig. 4A) and excitation (Fig. 4B) profiles and least-squares analysis assuming a biexponential decay. The nonlinearity of the log plot of the decay in Fig. 4A indicates that at least two exponential components are necessary, while the residuals of the analysis (Fig. 4C) indicate that two exponential components are sufficient to parameterize the decay. Owing to the large difference in time scales between excitation and emission events, deconvolution did not have a significant influence on the least-squares analysis. Decay curves were therefore routinely analyzed without deconvolution, using the expressions for $I_M(t)$ and $I_D(t)$ in Eqns. 9 and 10 as the ideal curves and k_M, k_D, k_{MD} and $k_{DM}c_M$ as the adjustable parameters. Values of the amplitudes, A_1 and A_2, and lifetimes, T_1 and T_2, were calculated according to Eqns. 8 and 9.

The biexponential character of the decay in Fig. 4 is typical of the decays we observed in all of the lipids we studied. The major part of pyrene molecular fluorescence in membranes arises from a component with a lifetime in the region of 100–200 ns and the remainder of the decay arises from a component with a lifetime in the region of 25–50 ns. The relative amplitude of the fast phase is not reproducible, and varies somewhat between different lipid types and on different days in the same lipid. Typically, the contribution of the fast phase is 10–20% when the pyrene concentration is 1 mM, but we have observed it to be as low as 5%. Table II is a compilation of rate parameters obtained for pyrene in membranes in the present study as well as in previous studies in other laboratories. A 100–200 ns lifetime component has been reported whenever pyrene fluorescence kinetics have been studied in membranes, and Dembo et al. [7] have also observed a 29 ns lifetime component in red cell ghosts at 25°C. Lianos et al. [21] reported that pyrene molecular fluorescence decay was well parameterized by a single exponential decay component in egg PC under unspecified conditions, whereas in studies on a number of different lipids Vanderkooi and Callis [5] observed nonexponential fluorescence decays, and a lack of appreciable concentration dependence of the molecular decay kinetics is also evident in their data.

Fig. 5A and B show the concentration dependences of the lifetimes of the fast and slow decay

TABLE II

PYRENE FLUORESCENCE KINETIC PARAMETERS IN MEMBRANES

Membrane type	T (°C)	k_M^{-1} (ns)	k_D^{-1} (ns)	k_{DM} (10^7 M^{-1}·s^{-1})	Ref.
Egg yolk PC	24	–	20	0.01	9,11
	20	–	–	2.2	5
	25	113	–	–	21
Soya bean asolectin	20	146 ± 10	45 ± 3	≤ 0.1	[a]
Dimyristoyl PC	30	135	–	2.2	5
Dipalmitoyl PC	45	–	100	4.2	6
Soya bean PC	20	100 ± 1	34 ± 2	≤ 0.1	[a]
Thylakoid PC	20	136 ± 10	37 ± 4	≤ 0.1	[a]
Erythrocytes	25	155	–	2.1	5
	25	182	29 [b]	4.4	7
	40	143	21 [b]	11.0	7
Sarcoplasmic reticulum	20	–	–	4.4	5
Thylakoid polar lipids	20	147 ± 12	40 ± 1	≤ 0.1	[a]

[a] This study.

[b] $(k_D + k_{MD})^{-1}$.

components and the amplitude of the fast component for pyrene in thylakoid PC liposomes. It is evident in Fig. 5A that neither of the lifetimes is concentration-dependent within the experimental error in the concentration region 10^{-3}–0.1 M pyrene. The amplitude of the fast component shows a significant increase, from 20–25% at 10^{-3} M pyrene to 40–50% at 0.1 M pyrene.

Let us assume for the sake of argument that the two components of the decay in Fig. 5A correspond to the two phases of the decay of a homogeneous pyrene population, consistent with Table I. A series of theoretical curves are presented in Fig. 6 which were calculated with the molecular fluorescence lifetime, k_M^{-1}, set equal to the average value of the slow phase lifetime in Fig. 5A, 136 ± 10 ns, and the excimer lifetime, k_D^{-1}, set equal to the average value of the fast phase lifetime, 37 ± 4 ns. Curves were calculated for the cases $k_{DM} = 10^8$, 10^7 and 10^6 $M^{-1} \cdot s^{-1}$, with $k_{MD} = 10^6 \cdot s^{-1}$. The concentration invariance in Fig. 5A of both lifetimes and the non-zero value of the fast-phase lifetime, when compared to the theoretical trends in Fig. 6A, suggests that the excimer formation rate constant, k_{DM}, is not larger than about 10^6 $M^{-1} \cdot s^{-1}$. Linear regression of the data in Fig. 5A using Eqn. 11 yields a negative value of k_{DM} as result of the apparent increase in lifetime of the slow phase. This increase is not reproducible, and the average value of the slope from three experiments in thylakoid PC is smaller than the experimental error in Fig. 5A. Similar results were obtained in all the lipid systems we studied.

To be consistent with the concentration invariance of both lifetimes, the amplitudes should have their asymptotic values $A_1 = 1$ and $A_2 = 0$, clear in the theoretical trend in Fig. 6B. Instead, the molecular fluorescence decay in Fig. 5B is substantially biphasic over the region 10^{-3}–0.1 M pyrene. We could find no set of rate parameters which would account for the concentration dependences of the amplitudes and lifetimes in terms of the model in Table I in any lipid system we studied. Thus the assumption that the slow and fast decay components correspond to the two phases of molecular fluorescence decay in Table I leads to inconsistencies, and we conclude that the theory of collisional excimer formation in Table I does not describe pyrene fluorescence kinetics in membranes.

Concentration studies of steady-state molecular and excimer fluorescence. Fig. 5C shows the concentration dependence of the steady-state excimer/molecular fluorescence ratio, I'/I, for pyrene in thylakoid PC liposomes. I' and I were measured at the respective emission maxima at 470 and 398 nm. In Fig. 5C, I'/I increases from 0.1–0.2 at 10^{-3} M pyrene to 0.4–0.6 at 0.1 M pyrene. The theoretical curves for I'/I in Fig. 6C were obtained using Eqn. 14 of Table I and the

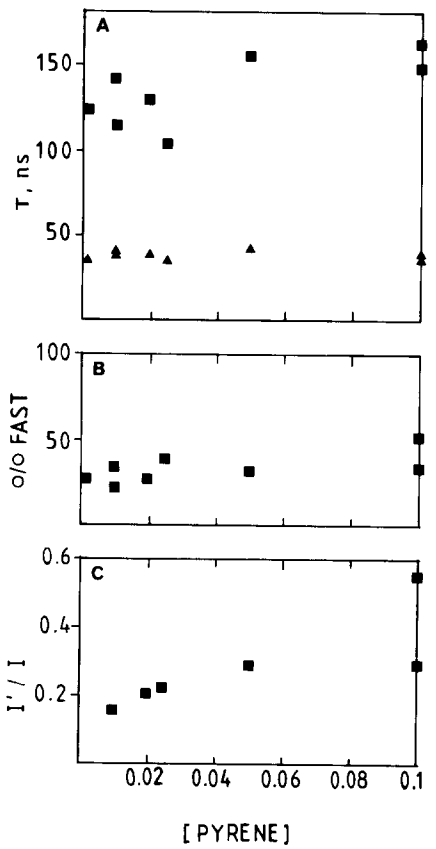

Fig. 5. Experimental concentration curves for pyrene molecular fluorescence parameters in aqueous dispersions of thylakoid PC. A: concentration dependences of the lifetimes obtained from least-squares analysis of molecular fluorescence decay assuming two exponential components. B: concentration dependence of the amplitude of the shorter lifetime component obtained from least-squares analysis. C: concentration dependence of the excimer/monomer fluorescence intensity ratio from measurements of steady-state fluorescence emission. Steady-state intensities were measured at 470 nm for excimer and 398 for monomer emission. Other measurement conditions were the same as in Fig. 3.

same assumptions as for Figs. 6A and B, plus the assumption that k_{1M} and k_{1D} in Eqns. 2 and 5 are independent of the solvent, as was suggested by Birks and coworkers [1–3]. Linear regression of the data in Fig. 5C using Eqn. 14 and the same set of assumptions yields a value of $2.6 \cdot 10^7\ M^{-1} \cdot s^{-1}$ for k_{DM}. This value is consistent with values obtained from previous studies of I'/I, which are typically in the region $(2–4) \cdot 10^7\ M^{-1} \cdot s^{-1}$.

The relation between time-dependent and steady-state pyrene fluorescence. The value of k_{DM} calculated from Eqn. 11 and fluorescence lifetime data is clearly incompatible with the value calculated above from Eqn. 14 and steady-state fluorescence data. We believe that the explanation for the inconsistency between the kinetic and steady-state fluorescence data, as well as the inconsistency between the concentration invariance of the lifetimes and the biphasicity of the decays, is that the excimer fluorescence observed in membranes comes from a population of pyrene molecules which gives rise to the fast molecular decay component and that the slow component arises from a different population of pyrene molecules. This view is supported by the high degree of correlation between the amplitude of the fast phase and I'/I. For the data in Fig. 5B and C we calculated a correlation coefficient of 0.85 between I'/I and the amplitude of the fast component, corresponding to a probability of less than 5% that I'/I and

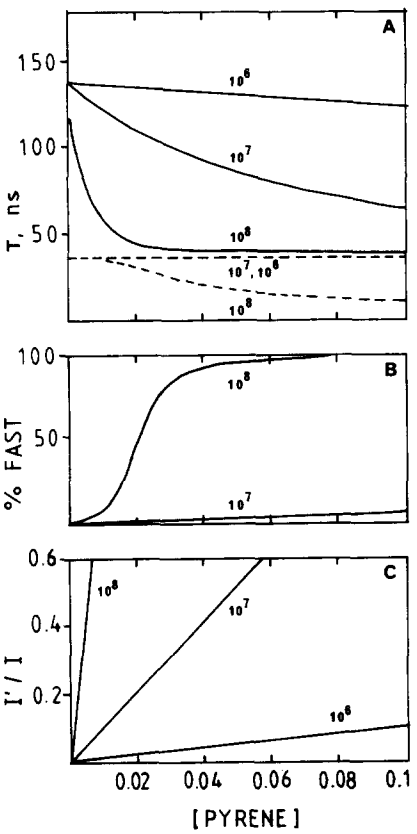

Fig. 6. Concentration curves for pyrene molecular fluorescence parameters at three different values of the excimer formation rate constant k_{DM} using the theoretical model in Table I. A: concentration dependences of T_1 (solid curves) and T_2 (dashed curves) calculated using Eqn. 8. B: concentration dependences of the amplitude of the fast phase A_2 calculated using Eqn. 9. C: concentration dependence of the excimer/monomer fluorescence intensity ratio calculated using Eqn. 14. The values assumed for k_{DM} are indicated in the figure. The other three parameters had the values $k_M^{-1} = 136$ ns, $k_D^{-1} = 37$ ns, and $k_{MD} = 10^6\ s^{-1}$.

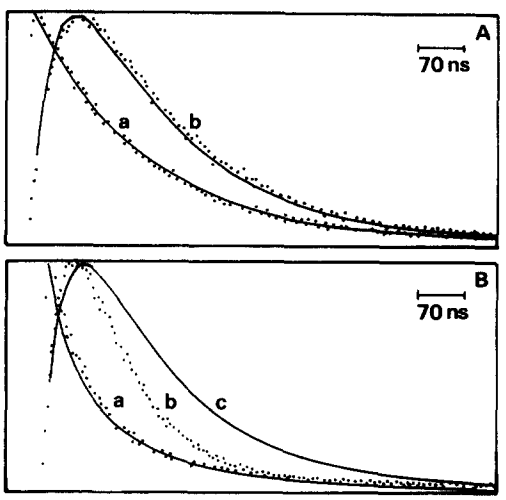

Fig. 7. Molecular and excimer fluorescence kinetics. A: 1 mM pyrene in absolute ethanol. (a) dots, molecular fluorescence decay data; solid line, best-fit curve from nonlinear least-squares analysis; (b) dots, excimer fluorescence data collected from the same sample; solid lines, excimer kinetics predicted using the best fit parameters from the analysis for curve (a). B: 1 μM pyrene in an aqueous dispersion of 0.05 mg·ml^{-1} thylakoid PC. (a) dots, molecular fluorescence decay data; solid line best-fit curve from least-squares analysis of molecular decay; (b) excimer fluorescence data collected from the same sample; (c) excimer kinetics predicted using the best-fit parameters from the analysis for curve (a). Excimer fluorescence was measured at 480 nm. Other measurement conditions were the same as for Fig. 3.

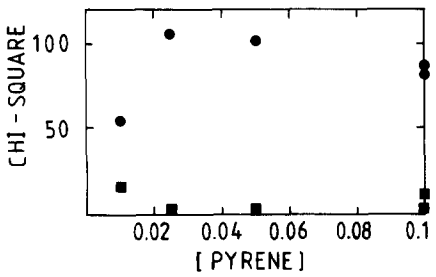

Fig. 8. The quality of theoretical fits to experimental molecular and excimer fluorescence kinetics for pyrene in aqueous dispersions of thylakoid PC. ■, values of reduced chi-square for the best-fit curve from least-squares analysis of molecular fluorescence decay; ●, values of reduced chi-square for the fit of the excimer kinetics predicted using the best-fit parameters from the analysis of the molecular fluorescence decay to excimer fluorescence data collected from the same sample.

the fast component are uncorrelated [22]. Naturally, this corresponds to a negative correlation between I'/I and the amplitude of the slow component.

Additional support for this view is presented in Figs. 7 and 8. Fig. 7A shows molecular and excimer fluorescence data we obtained for 1 mM pyrene in absolute ethanol. The solid curve through the data points in curve (a) is the theoretical curve obtained by nonlinear least-squares analysis of the molecular decay. The solid line in curve (b) is the excimer fluorescence kinetics predicted using Eqn. 12 and the best-fit parameters for the molecular decay in curve (a). The agreement between predicted and observed excimer kinetics was as good at all pyrene concentrations we studied in organic solvents. Fig. 7B shows the molecular and excimer fluorescence kinetics we observed for pyrene in model membranes of thylakoid PC. The parameters which gave the best fit to the molecular decay (curve (a)) predicted slower excimer kinetics (curve (c)) than those actually observed (curve (b)). The computed value of $k_{DM}c_M$ in Fig. 7B is lower for the molecular decay than it is for the observed excimer kinetics, consistent with the value of k_{DM} calculated from Fig. 5A and Eqn. 11 being lower than the value calculated from Fig. 5C and Eqn. 14. Fig. 8 shows that parameters which produce a fairly good fit to the molecular fluorescence data result in a very poor fit to excimer data collected from the same sample. Thus, it is clear that molecular and excimer fluorescence cannot be characterized by the same set of kinetic parameters.

Discussion

The results presented in this paper suggest that pyrene fluorescence kinetics do not satisfy the criteria for collisional excimer formation summarized in section 'Experimental tests for diffusion control'. First, the substantial biphasicity of the molecular fluorescence decay is clearly inconsistent with the theoretical model of collisional excimer formation. Second, the concentration curves for the lifetimes require a value for k_{DM} which is clearly different from the value required by the concentration dependence of I'/I, suggesting that molecular fluorescence and excimer formation are uncoupled. The latter conclusion is also supported by the finding that molecular and excimer fluorescence kinetics are characterized by different kinetic parameters. Our results indicate a heterogeneity in the distribution of pyrene in liposomes and a static rather than a collisional mechanism of excimer formation. We assign the two phases of molecular fluorescence kinetics to the values of T_1 for two separate populations of pyrene molecules, as follows.

The slow phase of molecular fluorescence decay

The slow phase of molecular fluorescence appears to arise from a population of pyrene molecules which do not undergo significant excimer formation in membranes up to concentrations of 0.1 M. We would assign the slow phase of pyrene molecular fluorescence decay to a population of monomeric pyrene molecules which undergo diffusion in the membrane with a high activational barrier and for which k_{DM} is less than or of the order 10^6 $M^{-1} \cdot s^{-1}$. Thus at pyrene concentrations up to 0.1 M, the conditions at the low concentration asymptote in Table I would apply, and the slow phase lifetime would correspond to the molecular fluorescence lifetime. The values of the slow phase lifetime obtained in a number of laboratories are consistent and it would seem that, in membranes, k_M is in the region of $(0.55–1.0) \cdot 10^7$ s^{-1}. This suggestion is not unreasonable in that k_M has been found to be highly solvent-dependent, with room-temperature values ranging

from $0.2 \cdot 10^7$ s^{-1} in absolute ethanol to $1.3 \cdot 10^7$ s^{-1} in benzene [3].

We suggest that the reaction rate constant for collisional excimer formation in the membrane systems we studied corresponds to the diffusion limit [23] and has an upper limit of 10^6 $M^{-1} \cdot s^{-1}$. We estimated the value of the molecular collision parameter for pyrene in membranes to be in the region $6 \cdot 10^4$–$1 \cdot 10^6$ $M^{-1} \cdot s^{-1}$, and a value of k_{DM} in this region is consistent with the concentration invariance of T_1 in Fig. 5A. Our results are in agreement with those of Dorrance and Hunter [11], who reported that k_{DM} is roughly $1 \cdot 10^5$ $M^{-1} \cdot s^{-1}$ in aqueous dispersions of egg yolk PC. The low value of k_{DM} arises from the high activational barrier to diffusion in membranes as compared to organic solvents [11] and thus does not imply that the reaction is under chemical rather than diffusional control [23].

The fast phase of molecular fluorescence decay

The fast phase of molecular fluorescence appears to be associated with a population of pyrene molecules in a highly concentrated state, for which the conditions at the high concentration asymptote in Table I apply. We would assign the fast phase of molecular fluorescence decay to aggregated pyrene molecules. The fast component lifetime would correspond to k_D^{-1}, the value of T_1 at the high concentration limit. As shown in Table II, the values obtained in several laboratories are consistent and suggest that k_D is in the region $(2–5) \cdot 10^7$ s^{-1} in membranes. This is reasonable, because k_D is known to be solvent-dependent, with room-temperature values ranging from $0.89 \cdot 10^7$ s^{-1} in crystals to $2.3 \cdot 10^7$ s^{-1} in acetone [3].

The high degree of positive correlation between I'/I and the amplitude of the fast phase suggests that fast phase and excimer fluorescence in membranes arise from the same population of pyrene molecules. The fluorescence spectrum of aggregated pyrene would most likely be a superposition of molecular and excimer fluorescence and excimer formation would occur by a static rather than a collisional mechanism. In highly concentrated solutions, pure liquids and crystals, molecules can interact strongly and with sufficient overlap for excimer formation to occur without diffusion [3]. Two types of aromatic crystal lattice have been distinguished [3]: type B, in which there is a large degree of molecular overlap; and type A, in which overlap is relatively small. In both types of crystal, single molecules undergo excitation [3]. However, type B crystals give rise to pure excimer fluorescence, whereas type A crystals give rise to molecular fluorescence. Single crystals of pyrene have type B fluorescence properties, whereas pyrene microcrystals and powders are a mixture of molecular and excimer fluorescence. Since crystal defects or impurities also result in molecular fluorescence [3], pyrene aggregates in membranes would be more likely to have fluorescence properties intermediate between type A and type B crystals than those of pure pyrene crystals.

If the model in Table I is not applicable to pyrene excimer formation in membranes, then I'/I is not governed by Eqn. 14 and the data in Fig. 5C are unrelated to k_{DM}. I'/I shows an apparently linear dependence on the pyrene concentration, e.g. in Fig. 5, and this suggests a Stern-Volmer concentration dependence, as noted previously [4–6]. However, the concentration independence of the lifetimes is inconsistent with a Stern-Volmer quenching mechanism [24], and indeed an equilibrium or exchange between pyrene molecules in the monomeric and aggregated forms would also give rise to a Stern-Volmer-type concentration dependence of I'/I [24]. The value of the equilibrium constant for exchange between the monomeric and aggregated states, K_E, calculated by linear regression of the data in Fig. 5B, is 1.4 M^{-1}, whereas the value calculated from the data in Fig. 5C is 2.8 M^{-1}. These values are in reasonable agreement and are three orders of magnitude higher than the value of the equilibrium constant for diffusion-controlled pyrene excimer formation and dissociation, 10^{-3} M^{-1}, observed in organic solvents [3]. Both k_{DM} and k_{MD} should have higher activational barriers in membranes than in organic solvents owing to the activational barrier to diffusion, and the equilibrium constant for diffusion-controlled excimer formation should be solvent-independent, as pointed out by Birks [3]. Thus the high value of K_E in membranes provides further support for the conclusion that excimer fluorescence observed in membranes does not result from diffusion-controlled excimer formation.

We have considered the possibility that our

results reflect an artefactual situation in our experimental system but have not found plausible reason why this should be so. Firstly, our data strongly indicate that pyrene is always associated with lipid and therefore that aqueous pyrene does not contribute to the observed fluorescence. Secondly, under our experimental conditions we expect no polymorphic transitions to occur [16], and, with the exception of hydrogenated thylakoid PC, all the lipids we used are in the liquid crystalline phase at 20°C. Soya bean and egg yolk PCs show no phase transitions down to −15 to −30°C [25] and no phase transition has been observed in thylakoid membranes or total polar lipid extracts above −10°C [16,26]. Indeed, mono- and digalactosyldiacylglycerols, which account for 80% of the lipid in thylakoid extracts, have been shown by X-ray diffraction studies to have transitions at or below −30°C [27]. Therefore our results cannot reflect effects caused by thermotropic phase transitions in these lipids. Thylakoid PC with a trienoic content of about 65% is likely to be in the liquid crystalline phase at room temperature [25,28]. On the other hand, the hydrogenated thylakoid PC we used would be expected to be in the gel phase due to its high content of stearic and palmitic acid [28], but the results in this lipid were qualitatively the same as in all the other lipids we used. It thus appears that even if the lipid molecules are in the gel phase, which is well documented as interfering with diffusional processes [28], our data remain basically the same, making the argument that pyrene excimer formation results from collisional encounters even less likely.

Conclusion

The essential point we are making in this paper is that the type, composition and degree of unsaturation of the lipid we used made no qualitative difference to the results of pyrene fluorescence studies. We never observed any concentration dependence of the molecular fluorescence lifetimes in any of the lipid systems we studied, and we always observed biphasic decay kinetics. We conclude that excimer fluorescence in membranes arises from an aggregated form of pyrene and does not reflect diffusion-controlled excimer formation. Our results are consistent with the collisional excimer formation rate constant being of the order $10^6\ M^{-1} \cdot s^{-1}$ or less and this value is consistent with the value estimated in the Theoretical section for k_{DM} on the basis of the high activational barrier to diffusion in membranes [3,11]. It is not possible to observe concentration dependence of the rate parameters or diffusion-controlled excimer formation at concentrations achievable in membrane preparations when k_{DM} is so small, and thus pyrene excimer formation is not capable of reflecting changes in membrane microviscosity. This would explain the observation of Kleinfeld et al. [4] that large microviscosity changes caused by perturbing agents such as free acids and reflected in measurements of diphenylhexatriene fluorescence depolarization are not accompanied by any change in pyrene molecular/excimer fluorescence intensity ratios. The results presented here suggest that caution should be exercised in the interpretation of fluorescence data when pyrene or pyrene adducts are used in membrane systems.

Acknowledgements

We thank Dr. Stephen Zara for help with the microcomputers. M.F.B. was supported by the United States Department of Health and Human Services, National Research Service Award No. 5-F32-GM09815 from the National Institute of General Medical Sciences. We acknowledge support from the Agricultural and Food Research council, the Science and Engineering Research Council and the Royal Society.

References

1 Birks, J.B., Dyson, D.J. and Munro, I.H. (1963) Proc. R. Soc. A 275, 575–588
2 Birks, J.B., Lumb, M.D. and Munro, I.H. (1964) Proc. R. Soc. A 280, 289–297
3 Birks, J.B. (1970) in Progress in Reaction Kinetics (Porter, G., ed.), Vol. 5, pp. 181–272, Pergamon Press, Oxford
4 Kleinfeld, A.M., Dragsten, P., Klausner, R.D., Pjura, W.J. and Matayoshi, E.D. (1981) Biochim. Biophys. Acta 649, 471–480
5 Vanderkooi, J.M. and Callis, J.B. (1974) Biochemistry 13, 4000–4006
6 Galla, H. and Sackmann, E. (1974) Biochim. Biophys. Acta 339, 103–115
7 Dembo, M., Glushko, V., Aberlin, M.E. and Sonenberg, M. (1979) Biochim. Biophys. Acta 522, 201–211

8 Galla, H., Theilen, U. and Hartmann, W. (1980) Chem. Phys. Lipids 27, 199–219
9 Dorrance, R.C. and Hunter, T.F. (1972) J. Chem. Soc. Faraday Trans. I 68, 1312–1321
10 Dorrance, R.C. and Hunter, T.F. (1974) J. Chem. Soc. Faraday trans. I 70, 1572–1580
11 Dorrance, R.C. and Hunter, T.F. (1977) J. Chem. Soc. Faraday Trans. I 73, 1891–1899
12 Noyes, R.M. (1961) in Progress in Reaction Kinetics (Porter, G., ed.), Vol. 1, p. 128, Pergamon Press, London
13 Razi Naqvi, K. (1974) Chem. Phys. Lett. 28, 280–284
14 Bligh, B.G. and Dyer, W.J. (1959) Can. J. Biochem. Physiol. 48, 163–165
15 Kates, M. (1972) in Techniques in Lipidology: Laboratory Techniques in Biochemistry and Molecular Biology (Work, T.S. and Work, E., eds.), Vol. 3, pp. 398–401, North-Holland, Amsterdam
16 Gounaris, K., Mannock, D.A., Sen, A., Brain, A.P.R., Williams, W.P. and Quinn, P.J. (1983) Biochim. Biophys. Acta 732, 229–242
17 Chapman, D.J., De Felice, J.G. and Barber, J. (1983) Planta 157, 218–223
18 Newman, G.C. and Huang, C. (1975) Biochemistry 14, 3363–3370
19 Huang, C. and Thompson, T.E. (1974) Methods Enzymol. 32, 485–489
20 Jones, O.T. and Lee, A.G. (1985) Biochemistry 24, 2195–2202
21 Lianos, P., Mukhopadhyay, A.K. and Georghiou, S. (1980) Photochem. Photobiol. 32, 415–419
22 Bevington, P.R. (1969) Data Reduction and Error Analysis for the Physical Sciences, pp. 119–121, McGraw-Hill, New York
23 Levine, I.N. (1978) Physical Chemistry, International Student Edition, pp. 775–777, McGraw-Hill Kogakusha, Tokyo
24 Parker, C.A. (1968) Photoluminescence of Solutions, pp. 72–74, Elsevier, Amsterdam
25 Quinn, P.J. and Williams, W.P. (1978) Prog. Biophys. Mol. Biol. 34, 109–173
26 Barber, J., Ford, R.C., Mitchell, R.A.C. and Millner, P.A. (1984) Planta 161, 375–380
27 Shipley, A.G., Green, J.P. and Nichols, B.W. (1975) Biochim. Biophys. Acta 311, 534–544
28 Stubbs, C.D. and Smith, A.D. (1984) Biochim. Biophys. Acta 779, 89–137